Using Assembled 2D LiDAR Data for Single Plant Detection

David Reiser[1], Manuel Vázquez Arellano[1], Miguel Garrido Izard[2], Hans W. Griepentrog[1]
and Dimitris S. Paraforos[1]

[1]*University of Hohenheim, Institute of Agricultural Engineering, Garbenstr. 9, D-70599 Stuttgart, Germany*
[2]*Laboratorio de Propiedades Físicas (LPF)-TAGRALIA, Technical University of Madrid, Madrid 28040, Spain*
David.reiser@uni-hohenheim.de

Keywords: LiDAR, total station, single plant detection, point cloud, 3D, maize plants

Abstract: A 2D laser scanner was mounted on the front of the small 4-wheel autonomous robot with differential steering, in an angle of 30 degrees pointing downwards. The machine was able to drive between maize rows and collect timestamped data simultaneously. The position of the vehicle was tracked by a highly precise total station. The data of the total station and the laser scanner was fused to generate a 3D point cloud. This 3D representation was used to search for single plant positions, what could later be used for additional applications like single plant treatment and precision weeding. First all points belonging to the ground plane were removed. Afterwards outliers were filtered. For separating the resulting points, a k-d tree clustering was used. Of each single point cloud cluster the 3D centroid was evaluated and assumed as the resulting plant position. This was done on three different growth stages of the plants. Results showed good detection rates up to 70.7 % with a root mean square error of 3.6 cm, precise enough to allow single plant treatment.

1. INTRODUCTION

Detecting single plants can bring a big advantage to modern agricultural machinery like tractor attachments or fully autonomous robots. When the positions of plants are known precisely, variable rate applications can be scaled down to single plant treatments. This could help to decrease rapidly the use of chemicals, like fertilizers, pesticides, or fungicides. Also mechanical precision weeding is possible, when the exact position of the plants is known (Griepentrog et al. 2005). In order to perform safe and reliable autonomous navigation in agriculture, machines need robust object classification in the environment and adequate behavior to their appearance (Reina et al. 2015; Fountas et al. 2007). It's necessary to detect everything in the environment what can harm the robot, to find the right strategy for the navigation. Single plant detection could help to improve decisions if sensor data belongs to a rigid or flexible obstacle, or it is just noise. This information would make possible a much more robust path navigation

for future applications. Also obstacles like stones, holes, wires or wood sticks could be better detected.

Many of the autonomous outdoor robots today using 2D light emitting and ranging (LIDAR) laser scanners, which are still more robust and efficient for basic navigation than camera based systems (Hiremath et al. 2014; Steen et al. 2016). When the position of the sensor is known, 2D laser scanners can also be used to gain 3D information of the environment. When the sensor is moved on a known trajectory, or the vehicle movement is known precisely, this established sensor poses could be used to transform the sensor data to the same coordinate frame.

Detecting single plants was already researched relying on different sensors and strategies. Shrestha et al. used an Otsu thresholding algorithm to discriminate maize plants from weed in video data (Shrestha et al. 2004). Also sugar beet was analyzed for crop/weed discrimination using 2D images (Åstrand & Baerveldt 2004). Single outputs of a 3D-LIDAR scanner were analyzed by Weiss and Biber,

using a k-d-Tree algorithm, to discriminate between early stage maize plants with a detection rate of 60 % (Weiss & Biber 2011). This was done indoors and outdoors in an optimized test crop row. When using machine learning algorithms, the detection rate could be increased to 99 % with the use of a decision tree based Logistic model trees algorithm (Weiss et al. 2010). Garrido et al. used a LIDAR light curtain to detect stem positions of almond trees with a detection rate of 99.48 % (Garrido et al. 2014). The position of the detected stems was obtained with the help of an optical wheel odometer. Also, sonar sensors where used to detect plants, but the results were much less precise (Harper & McKerrow 2001). 3D-point clouds from sonar data was obtained by Martin et al. 2016 to detect artificial plants.

In general 3D representations can bring more advanced information than just the plant position, like plant height, leaf area, yield or even evaluations of plant health (Garrido et al. 2015). As Vázquez-Arellano et al. points out, it's necessary to have 3D sensor data to gain this information (Vázquez-arellano et al. 2016). But most of these sensors are still costly what make a commercial use unrealistic. So the best case would be to reuse sensors needed for navigation also for single plant detection, like a 2D LIDAR sensor, mounted at the front of an autonomous vehicle. This would help to reduce costs for advanced plant detection.

One common technique to detect objects in 3D point clouds on flat surfaces is first to reduce the ground plane, and then to cluster the remaining points. One fast and robust variant for the ground removal is to use of the Random sample consensus (RANSAC) algorithm (Fischler & Bolles 1981). For easy, fast and robust clustering the k-d tree method could be used (Bentley 1975).

The aim of this paper is to show that it is possible to use a terrestrial 2D LIDAR for obtaining 3D point clouds of maize plants by tracking precisely the position of the vehicle and using this information to detect single plant positions of early-stage maize. In order to obtain 3D information, data from a total station and an Inertial Measurement Unit (IMU) was fused. For plant detection in the dataset, a commonly used algorithm for object localization in 3D point clouds was applied. As the real plant positions were measured with a total station, it was possible to evaluate the precision of the detected positions.

The paper is structured as follows: in section 2.1 Hardware and sensors are mentioned. The software used for data acquisition is described in section 2.2, in section 2.3 the test environment is described. In the

section 2.4 the algorithm for single plant detection is explained in detail. In chapter 3, the results are evaluated, with detection rate and accuracy, comparing them with the provided reference. These results are discussed in the same section. Finally, the conclusion is given in chapter 4.

2. MATERIAL AND METHODS

1.1 Hardware and Sensors

A small 4-wheel autonomous robot with differential steering was the carrier vehicle to move the sensors through the crop rows (see Figure 1) (Reiser et al. 2015). A LMS111 2D-LiDAR laser scanner (SICK, Waldkirch, Germany) was used, mounted at a height of 0.58 m, pointing downwards at an angle of 30 degrees. To measure the robot orientation, the VN-100 Inertial Measurement Unit (IMU) (VectorNav, Dallas, USA), was included in the sensor setup. The robot position was evaluated by the SPS930 Universal Total Station (Trimble, Sunnyvale, USA). The total station tracked a Trimble MT900 Machine Target Prism, which was mounted on top of the robot at a height of 1.07 m (see Figure 1).
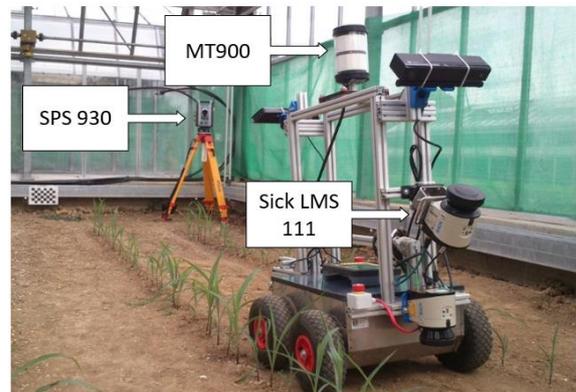

Figure 1. Equipped robot platform for the data acquisition

1.2 Software

The robot computer runs on Ubuntu 14.04 and uses the Robot Operating System (ROS-Indigo) middleware for sensor control and data recording. All the software components were programmed in a combination of C++ and Python programming languages. For fast calibration, point measurement and importing the total station data into ROS, the Trimble SCS900 Site Controller (Software Version

MCG 2016 – 5th International Conference on Machine Control & Guidance
"Facing complex outdoor challenges by inter-disciplinary research"
Vichy, France, October 5-6th, 2016

3.4.0) graphical interface was used. The prism position data was time stamped and helped to refer the transforms to the global frame and to interpolate the data.

1.3 Calibration and Experiments

For referencing to the same Cartesian coordinate frame in every test, 5 fixed points were defined nearby the test area (Reiser et al. 2015; Garrido et al. 2015). To relocate this points for every test, a greenhouse with a solid concrete wall was selected for the data acquisition. The precise position of these 5 points could be located by just screwing a prism of the total station on fixed positions on the concrete wall. With this positions, the positioning system of the total station could be calibrated to one fixed coordinate frame. The inaccuracy in the static measurement could be estimated by reassessing each of these fixed points with the first measurement. The shift between the first reference points and the actual measurements was in all tests below 4 mm for all three dimensions. For the robot rigid body frame, carrying the sensors, a static transformation between the prism and the sensor position was assumed. So first the roll, pitch and yaw angle of the IMU was fused together with the prism position and was used to create a coordinate frame for the prism position. After that, a static transformation to the robot geometric center and to the sensor position was performed. This procedure allowed to track down the precise sensor position and orientation in the same reference frame in every test (Reiser et al. 2015; Garrido et al. 2015). In Figure 2, the RGB image (a) and the assembled point cloud of the tilted laser scanner (b) of two crop rows is depicted.
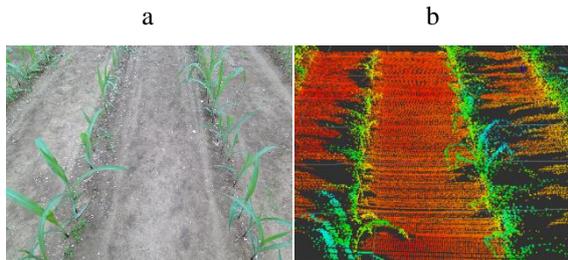
a b

Fig 2. Visualization of the assembled point cloud data of the tilted laser scanner at the dataset 2 (see Table I).

The spacing between the plants was defined by different Gaussian distributions for every crop row, to emulate diverse real scenarios. The rows used in this paper had a Gaussian distribution and a standard deviation of 0.015 m for the spacing. In total 41 plants were planted per row. The ground truth positions of the plants were measured using the total station just after emergence with the help of a tripod. The tests were performed in three different growth stages to compare the detection results.

After every test, the height of every single plant was manually measured. For the analysis of this test the data of just one row was used. All three tests were performed in the same direction, driving towards the total station. The laser scanner was always at the front of the driving direction.

1.4 Plant detection algorithm

To obtain an absolute reference of the plant positions, first the single scans were filtered, so that reflections of the vehicle and the greenhouse wall were removed from the sensor data. Also, the limits of the points were set to a defined distance, so that just one row to the left and one to the right of the robot could be observed. Just points in the range of 0.75 m to the left and 0.75 m to the right from the sensor position were considered. This filtered scans were transformed together with the fusion of the robot total station position and the IMU orientation together to a world coordinate system. With this new reference, all points could be transferred to one 3D point cloud, in a global world coordinate system. To detect the plants in this point cloud, first the ground was removed. The resulting points were filtered for the single plants and the positions were converted to a separate plant map to compare them with the ground truth (see Figure 3).

Firstly, the plant points had to be separated from the ground points. This was performed with a basic RANSAC plane algorithm as implemented in the PCL (Fischler & Bolles 1981). To get rid of noise and outliers, the remaining plant points were filtered with the use of a radius outlier filter (PCL 1.7.0, RadiusOutlierRemoval class). Afterwards, the results were clustered to define point cloud groups of every single plant. For separating the resulting points, a k-d-Tree clustering was used (PCL 1.7.0, EuclideanClusterExtraction class)(Bentley 1975; Rusu 2009) assuming that the plants were separated by a spatial gap in the point cloud by taking the 3-dimensional Euclidian point distance into account. For every single point cloud cluster the 3D centroid was evaluated and assumed as the resulting plant position. The centroid c is correlated to the number of n points p in one point cloud cluster in equation 1.

$$c = \frac{1}{n}\sum_{i=1}^{n} p_i \qquad (1)$$

Total Station | IMU | Laser Scanner

↓ 3D point cloud in global frame

Ground Detection (RANSAC)

↓ 3D point cloud without ground

Plant Detection
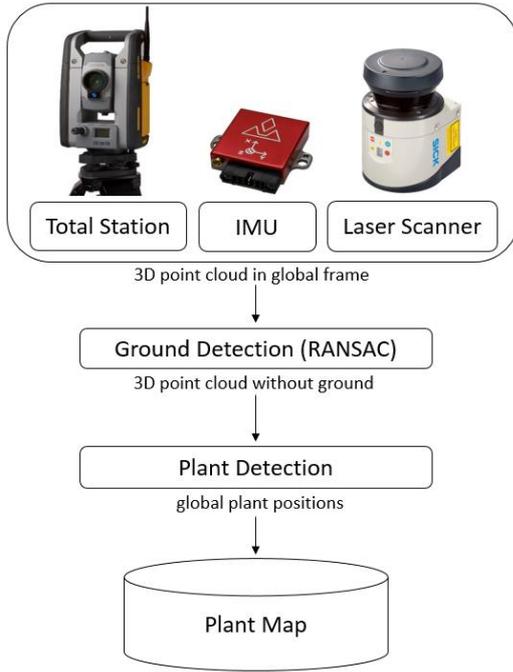
↓ global plant positions

Plant Map

Figure 3 basic flowchart of the plant detection process implemented in the software.

To be able to adjust the best parameters for the algorithm, they were adjusted for every row and test separately. All used parameters for the algorithm are listed for every test in Table II.

Just the x and y coordinates of the plants were considered for ground truth. The results of the algorithm for plant position detection was compared to the measured position by the total station to define the achieved precision (see also Table IV). For assessing the accuracy of the plant pose the Root Mean Square Error (RMSE) was used.

$$RMSE = \sqrt{\frac{\sum_{i=1}^{n}(\delta_i - \beta_i)^2}{n}} \qquad (2)$$

With δ_i as ideal plant position measured by the total station and β_i as the resolved algorithm plant position with the corresponding number i.

Table I: Description of used datasets and sensor data

Dataset [no.]	Days after seeding [d]	Date	Duration [s]	IMU data [no.]	Tilted laser scans [no.]	Total station data [no.]
1	26	21.4.2015	78	3146	1965	1573
2	28	23.4.2015	54.8	2189	1366	1086
3	32	27.4.2015	60	2426	1499	1200

Table II. Algorithm settings

Dataset [no.]	Row side	RANSAC distance [m]	Noise radius [m]	Minimal points inside radius [no.]	Cluster Distance [m]	Min cluster size [no.]	Max cluster size [no.]
1	Left	0.045	0.05	20	0.02	5	1000
1	Right	0.035	0.03	10	0.05	5	1000
2	Left	0.06	0.05	15	0.03	5	1000
2	Right	0.035	0.05	15	0.05	5	1000
3	Left	0.06	0.05	15	0.05	5	1000
3	Right	0.03	0.05	15	0.03	5	1000

Table III. Description of plant states in the rows

	left row			right row		
Dataset no.	average height [m]	Plant no.	standard deviation [m]	average height [m]	Plant no.	standard deviation [m]
1	0.14	41	0.0567	0.12	41	0.0556
2	0.17	41	0.0624	0.13	41	0.0609
3	0.23	41	0.0831	0.16	41	0.0786

Table IV. Algorithm results

Dataset no.	Row side	Correct detected Plants no.	Plants detected [%]	False positives [%]	Mean Distance [m]	Standard deviation [m]	RMSE [m]
1	Left	25	60.9	17.1	0.044	0.023	0.050
1	Right	28	68.2	2.4	0.030	0.020	0.036
2	Left	29	70.7	4.9	0.046	0.026	0.053
2	Right	20	48.8	2.4	0.037	0.019	0.042
3	Left	28	68.3	29.3	0.050	0.043	0.066
3	Right	25	61.0	4.8	0.052	0.040	0.065

In Figure 4, a processed point cloud is shown in a 3D representation of rviz (ROS-Indigo). The red spheres correlate to the automatically detected plant positions.
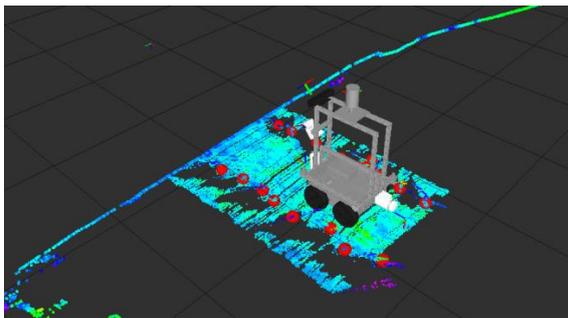

Figure 4 Representation of the algorithm in rviz. Assumed plant positions are depicted as red spheres.

3. RESULTS AND DISCUSSION

The used datasets were collected after 26-32 days after seeding. The details about number of laser scans, total station and IMU data, and duration of each test could be found in Table I. The plant height varied in average from 0.12 to 0.23 m in the test rows. During growth, also the standard deviation of the plant height increased for both sides. The details of the growth stages are listed in Table III.

The detection rate of the used algorithm achieved varying rates and reached up to 70.7%. The worst detection rate was around 48.8%. This was achieved with even quite sufficient precision, with a best standard deviation of 0.02 m and a RMSE of 0.036 m at the right row of test no. 1 (see also Table IV). The false positive rate of this test is very small with an amount of 2.4%. The accuracy of this test is basically determined by the measuring accuracy of the laser scanner, what would make a more accurate result difficult to achieve. The percentages were calculated in correlation with the 41 plants at every single row.

When looking at the results of Table IV, it's detectable, that the accuracy decreases with the growth stage of the plants. Thus, increasing the RMSE on the right row from 0.036 m to 0.065 m, and from the left row from 0.05 m to 0.065 m over the tests. Some explanations for that could be that as the plants grow, they have more leaves hanging in the

line of sight, causing some plant poses being detected at single leaves. This can be related to the low point density of the point clouds, leading to several wrong departed clusters of the same plant. This produced false positives, or double plant detection. Also, sometimes two plants could not be separated because of the close distance between them, leading to the detection of one plant directly in the middle of two real ones.

The detection rate of the algorithm was quite low, but was mainly due to the height growth diversity of the plants. That caused, on many parts, that small plants were shadowed by the bigger ones beside them. In areas of low height variability, the detection rate was much higher and much more accurate. The detected positions of 3 plants in reference to the global frame, are shown in Figure 5. Here, it could be seen, on all 3 datasets, a good detection precision.

The precision on small plants was considerably good, where some plants had a detection rate of 100% over all 3 tests, with a high precision in the position of some of them (less than 3 cm deviation), making the detection rate good enough to allow single plant treatment or mechanical weeding.
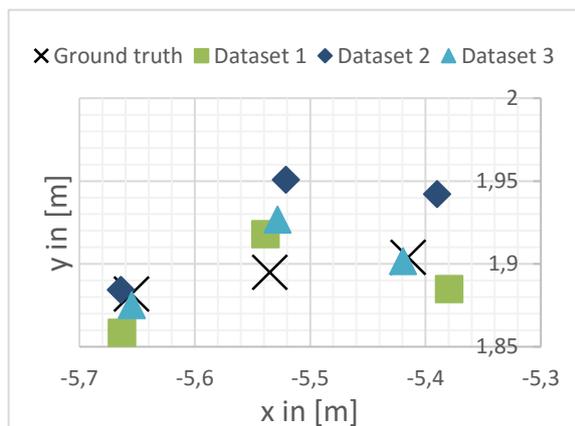

Figure. 5: Details of 3 plant positions and the tree positions detected by the algorithm.

The biggest challenges of the algorithm settings, was the discrimination between ground and plant points. Especially when the plants are small, the height difference was not enough to use a simple RANSAC plane filter. For that, in future research it could be helpful to discriminate ground and plant points not only by using a plane model, but also taking into consideration the laser intensities. Another option could be to separate the point clouds in smaller sub clouds, where the ground is separated from the plant points, without taking just one plane equation for the whole row. So the overall flatness of the test area would not be important for the outcome of the algorithm.

Another impact point was the density of the point cloud, where just parts of a leaf were covered by the laser beams. This caused that such a leaf could not be related to the right plant. To solve this, more complex plant models should be used for the point cloud clustering. Also, driving several times through the same row and matching the point clouds together could help to reduce this problem by increasing the density of the point could.

In general, the described method could be able to perform also in other growth stages, as long as the plants can be separated in single point cloud clusters, which is dependent on point cloud density and plant spacing. In the best cases, the plants stand completely isolated and can be easily distinguished from other plants, ground or weeds.

As long as the objects of interest are clearly separated, like in early stage maize, the introduced method promises good results. For real and reliable detection of maize plants, other algorithms such as machine learning algorithms, or fusion with 2D image analysis must be used to make detection rates up to 100 % possible. The investigation of better methods for plant to ground separation algorithms seems to be necessary. With the use of other algorithms like a region growing or by the use of normal orientations for the clustering, better results could be achieved. Also, intensities and multiple echoes of LIDAR sensors can be used for better classification (Reymann et al. 2015).

4. CONCLUSION

A 2D LIDAR laser scanner was used to collect 3D point clouds with the use of a total station and an IMU. This point clouds were collected at three different growth stages and were used to detect single plant positions of maize. For plant detection, first the ground was removed with the use of a RANSAC plane fitting algorithm. Afterwards, the results were filtered with a radius outlier filter. The resulting points were clustered with a k-d tree based Euclidean clustering. The centroid was solved for every point cloud cluster, thus considering it as the detected plant position. The results of the test showed good performance and high detection rate at clearly separated plants in early grow stages, which made possible the precise detection of the plant position for additional tasks. The plant detection was faulty at middle and late growth stages due to multiple reasons

such as hanging leaves in the area of the neighboring plant, shaded plants and undetected spatially close plants.

References

Åstrand, B. & Baerveldt, A., 2004. Plant recognition and localization using context information. In *IEEE Conference Mechatronics and Robotics 2004 special sessions Autonomous Machines in Agriculture*. Aachen, Germany, pp. 1191–1196.

Bentley, J.L., 1975. Multidimensional Binary Search Trees Used for Associative Searching. *Communications of the ACM*, 18(9), pp.509–517.

Fischler, M. a & Bolles, R.C., 1981. Random Sample Consensus: A Paradigm for Model Fitting with Applications to Image Analysis and Automated Cartography. *Communications of the ACM*, 24, pp.381–395.

Fountas, S. et al., 2007. Decomposition of agricultural tasks into robotic behaviours. *Agricultural Engineering International: the CIGR Ejournal. Manuscript PM 07 006*, IX.

Garrido, M. et al., 2015. 3D Maize Plant Reconstruction Based on Georeferenced Overlapping LiDAR Point Clouds. *Remote Sensing*, 7(12), pp.17077–17096. Available at: http://www.mdpi.com/2072-4292/7/12/15870.

Garrido, M. et al., 2014. Active optical sensors for tree stem detection and classification in nurseries. *Sensors (Basel, Switzerland)*, 14(6), pp.10783–10803.

Griepentrog, H.W. et al., 2005. Seed mapping of sugar beet. *Precision Agriculture*, 6(2), pp.157–165.

Harper, N. & McKerrow, P., 2001. Recognising plants with ultrasonic sensing for mobile robot navigation. *Robotics and Autonomous Systems*, 34(2-3), pp.71–82. Available at: http://linkinghub.elsevier.com/retrieve/pii/S0921889000001123.

Hiremath, S.A. et al., 2014. Laser range finder model for autonomous navigation of a robot in a maize field using a particle filter. *Computers and Electronics in Agriculture*, 100, pp.41–50. Available at: http://www.sciencedirect.com/science/article/pii/S0168169913002470 [Accessed February 4, 2014].

Reina, G. et al., 2015. Ambient awareness for agricultural robotic vehicles. *Biosystems Engineering*, (Robotic Agriculture), pp.1–19.

Reiser, D. et al., 2015. Crop Row Detection in Maize for Developing Navigation Algorithms under Changing Plant Growth Stages. In V. M.-M. Luís Paulo Reis, António Paulo Moreira, Pedro U. Lima, Luis Montano, ed. *Advances in Intelligent Systems and Computing*. Lisbon: Springer, pp. 371–382.

Reymann, C. et al., 2015. Improving LiDAR Point Cloud Classification using Intensities and Multiple Echoes. In *IEEE/RSJ International Conference on Intelligent Robots and Systems (IROS)*. Hamburg, pp. 5122–5128.

Rusu, R.B., 2009. *Semantic 3D Object Maps for Everyday Manipulation in Human Living Environments*. Technische Universität München.

Shrestha, D.S., Steward, B.L. & Birrell, S.J., 2004. Video processing for early stage maize plant detection. *Biosystems Engineering*, 89(2), pp.119–129.

Steen, K.A. et al., 2016. Using Deep Learning to Challenge Safety Standard for Highly Autonomous Machines in Agriculture. *Journal of Imaging*, pp.2–9.

Vázquez-arellano, M. et al., 2016. 3-D Imaging Systems for Agricultural Applications — A Review. *Sensors*, 16(618), p.24.

Weiss, U. et al., 2010. Plant species classification using a 3D LIDAR sensor and machine learning. *Proceedings - 9th International Conference on Machine Learning and Applications, ICMLA 2010*, pp.339–345.

Weiss, U. & Biber, P., 2011. Plant detection and mapping for agricultural robots using a 3D LIDAR sensor. *Robotics and Autonomous Systems*, 59(5), pp.265–273. Available at: http://linkinghub.elsevier.com/retrieve/pii/S0921889011000315 [Accessed July 26, 2012].